ELECTROSTATIC MEANS FOR INTRUSION DETECTION AND RANGING

Alan D. Aronoff, et al

Frankford Arsenal
Philadelphia, Pennsylvania

1965

ARONOFF, BOGHOSIAN and
JENKINSON

ELECTROSTATIC MEANS FOR INTRUSION DETECTION AND RANGING

ALAN D. ARONOFF, MR.
WILLIAM H. BOGHOSIAN, DR.
HOWARD A. JENKINSON, MR.
FRANKFORD ARSENAL
PHILADELPHIA, PA

INTRODUCTION

Electrostatic intrusion detection techniques have been utilized in the past for a variety of applications, both military and civilian. The basis for these techniques has been essentially the measurement of the distortion of an electric field due to the presence and/or motion of an object. An equivalent point of view results from analyzing the electric field perturbations in terms of the self and mutual capacitances of the detector probe and the object, and the variations of these capacitances with changes in the relative location of the detector and object.

A passive electrostatic detection system is one in which the electric field is generated external to the detector or sensor. If, however, the sensor itself generates the electric field which is perturbed by the object, the system is known as an active electrostatic detector. In this paper we deal with a passive detection system in which the earth's electric field, which is normally directed vertically to the earth's surface, is perturbed or distorted by the presence of an intruder.

The magnitude of the distortion depends on the relative position of the intruder and sensor and the configuration and dimensions of both. Fig. 1a shows the undisturbed field with the sensor depicted as a probe or antenna of arbitrary shape connected to a meter. It is assumed that probe size and shape are such that it does not disturb the field being measured. Fig. 1b shows the field distorted by the presence of an intruder modelled in this case as a grounded conductor.

The entire intrusion detection system is shown in block diagram form in Fig. 2.

The above model represents an oversimplification of the effect of a walking intruder on the earth's electric field. Such an intruder cannot be represented simply as a moving grounded conductor. A person walking or scuffing may develop potentials of over 1000 volts depending on shoe sole thickness and resistance and on the nature of the ground surface and material. Moreover, as he raises one foot at each step his body capacitance to ground reaches a minimum and this in turn causes his potential to rise to a maximum. When both feet are momentarily making ground contact, the charge potential is lowest, and, thus, there results a characteristic rise and fall in potential due to walking. This in turn introduces a similar disturbance in the earth's field in the vicinity of the moving person. This phenomenon is readily observed experimentally and it can be shown that the charge-discharge phenomena of a walking person will produce significant signals at useful ranges.

This paper is based on the results of an initial study to determine the feasibility of a reliable, reasonably inexpensive electrostatic intrusion detection system for field use. This initial effort has been concerned mainly with carrying out an analytic program through modelling and computer studies together with a preliminary experimental program based on these studies. In subsequent effort it is intended to expand these studies to include signal processing techniques required for the optimization of the detection and identification performance of the system and, in addition, breadboard components suitable for application of this detection technique to scatterable mine systems.

MODEL STUDIES

In this section we will first consider distortions in the earth's electrostatic field due to grounded and charged intruders. We will next introduce a time dependence due to motion toward the sensor as well as the charge/discharge phenomena attributable to the raising and lowering of the intruder's feet. We then outline a system capable of detecting these distortions through atmospheric coupling. The effects of finite input resistance and non-zero input capacitance of the detector are also accounted for.

To determine the distortion, which we define as the difference in the field due to the presence of an intruder after subtracting out the naturally occurring earth's field, it is necessary to solve Laplace's equation in a geometry appropriate to that of the intruder.

If the intruder is modelled as a conducting surface of constant value in some orthogonal coordinate system in which the Laplacian operator separates into ordinary differential operators, then it is not too difficult to obtain a closed form analytic solution.

We first consider analytic solutions for some simple geometries which approximate the intruder. The simplest of all is the grounded hemisphere (Fig. 3). It is well known that the potential outside and above a grounded hemispherical boss on a infinite grounded plane in a uniform electric field is given by[1]

$$V(\rho,z) = E_o z \left\{1 - a^3 (\rho^2+z^2)^{-3/2}\right\}, \quad a = \text{radius of boss} \qquad (1)$$

where E_o is the constant, undisturbed earth's electric field, 100 v/m in this calculation.

However, the hemisphere is a rather poor model since it implies that the intruder is as wide as he is tall. A much better model is a grounded hemiprolate-spheroidal (half watermelon) boss on the infinite plate (Fig. 4). By switching to the prolate spheroidal coordinate system ζ, η defined by the transformations:

$$\rho^2 (\eta^2-1)^{-1} + z^2/\eta^2 = C_2^2 \qquad (2)$$
$$\rho^2 (\zeta^2-1)^{-1} + z^2/\zeta^2 = C_2^2 \qquad (3)$$

where C_2 is determined from the semi-major axis, C, and semi-minor axis, b, of the spheroid by $C_2 = \sqrt{C^2-b^2}$, it can be shown[1] that V is now given by

$$V = E_o z \left[1 - \frac{\frac{1}{2}\ln((\eta+1)/(\eta-1)) - 1/\eta}{\frac{1}{2}\ln((\eta_o+1)/(\eta_o-1)) - 1/\eta_o}\right], \qquad (4)$$

where $\eta_o = C/C_2$. In these models we used b = 0.15 m and C = 2.0 m which approximate the dimensions of a man.

There are other models which may represent limiting values for the intruder. For example, we considered the grounded, half-elliptic cylinder of semi-major axis C and semi-minor axis b, shown in Fig. 5. The solution of Laplace's equation for this geometry can be shown to be[2]:

$$V = E_o z \left\{1 - \frac{\eta_o (\eta_o + \sqrt{\eta_o^2-1})}{\eta(\eta+\sqrt{\eta^2-1})}\right\} \qquad (5)$$

where η and η_o are the same as in the above prolate spheroid (Eqns. 2 and 3).

We can also consider the generalized ellipsoid with no axial symmetry (Fig. 6). Following Jeans[3], if one has the ellipsoid

$$x^2/a^2 + y^2/b^2 + z^2/c^2 = 1 \qquad (6)$$

then the conicoid

$$x^2(a^2+\theta)^{-1} + y^2(b^2+\theta)^{-1} + z^2(c^2+\theta)^{-1} = 1 \qquad (7)$$

will be confocal to the ellipsoid for all values of θ.

Solving the cubic equation for θ gives the three values λ, μ, υ for each cartesian point x, y, z where λ = const. is a family of ellipsoids, μ = const. is a hyperboloid of one sheet, and υ = const. is a hyperboloid of two sheets. If we require $a > b > c$, and assume the field is in the x direction, it can be shown that

$$V = E_o x\left[\int_{\lambda_o}^{\lambda} \frac{d\lambda}{(a^2+\lambda)\Delta_\lambda}\right] \Big/ \int_{\lambda_o}^{\infty} \frac{d\lambda}{(a^2+\lambda)\Delta_\lambda} \qquad (8)$$

where λ_o is the coordinate of the intruding ellipsoid of height a, length b, and breadth c, and

$$\Delta_\lambda = \sqrt{(a^2+\lambda)(b^2+\lambda)(c^2+\lambda)}.$$

Thus, the integrals in Eqn. (8) are of the form

$$I = \int d\lambda \left[(a^2+\lambda)^3(b^2+\lambda)(c^2+\lambda)\right]^{-\frac{1}{2}} \qquad (9)$$

which can be evaluated in terms of appropriate elliptic integrals of the first and second kinds[4].

We have plotted the field distortions of the prolate spheroid and elliptic cylinder geometries in Fig. 7. The field distortion was obtained directly from the potential distribution matrix V(i,j), where V(i,j) represents the potential at the point Z(i) and ρ(j) and then using a central difference formula to approximate the gradient operator:

$$E_z(i,j) = (\Delta z)^{-1}\{V(i+1,j) - V(i-1,j)\} - E_o \qquad (10a)$$

$$E_\rho(i,j) = (\Delta\rho)^{-1}\{V(i,j+1) - V(i,j-1)\} \qquad (10b)$$

where $\Delta z = [z(i+1) - z(i-1)]$ and $\Delta\rho = [\rho(j+1) - \rho(j-1)]$.

It is noted that the horizontal components of the field distortion are much smaller than the vertical components, except perhaps at points very close to the intruder. Furthermore, at horizontal distances from the intruder greater than 3 m , E_{hor} is proportional to the height off the ground, while E_{vert} is almost height independent. It would then seem desirable to detect the vertical component, taking advantage of these two important features.

Note further that the distortions for the elliptic cylinder are much stronger and fall off slowly as a function of ρ. Thus, we

put this as a maximum upper bound for the distortion due to a grounded object of elliptical cross section.

It is an oversimplification, however, to assume that the intruder remains at ground potential. For example, an initially grounded, conducting intruder has a charge distribution induced on his surface by the external field to enable him to remain at ground potential. Should the intruder break the connection to ground by lifting his feet, he reduces his capacity to ground which increases his potential. A similar if weaker effect occurs when the intruder picks each leg up, especially if his resistance to ground is not particularly high. Furthermore, scuffing shoes on the ground can lead to static charge being accumulated on the body, which must leak away in a finite time. The amount of charging is not inconsiderable. Over 20 years ago the Bureau of Mines[5] investigated the hazard of static electricity in operating theaters where there was danger of igniting explosive anesthetics. In a very comprehensive study it was shown that, depending upon the nature of the clothes, linens, furniture surfaces, shoes, and humidity in the room, potentials of 500-18000 volts could be generated on human beings. This charge leaked away through shoes with resistance of 10^5-10^9 ohms depending on the shoe material, which varies from partially conducting leather to highly insulating rubber. The time dependence of the potentials was also considered in that report. Thus, it becomes very necessary to obtain the field distortion due to a charged body. For this calculation we assume that the charged body is sitting on a thin insulating pad just above the ground.

Since the ground plane is at zero potential, one may resort to the theory of images to solve this problem. The application of this method to a charged conducting hemisphere on a ground plane leads to the well known exterior solution

$$V(r,\theta)=V_0\left[3/2\left(\frac{a}{r}\right)^2P_1(\cos\theta)-7/8\left(\frac{a}{r}\right)^4P_3(\cos\theta)+(11/16)\left(\frac{a}{r}\right)^6P_5(\cos\theta)--\right] \quad (11)$$

where $P_i(\cos\theta)$ is the Legendre polynomial of the first kind. Again while the sphere is not a good approximation to the man, we can still use the same technique to solve the problem of the charged conducting prolate ellipsoid.

The general solution of the Laplacian in prolate spheroidal coordinates with azimuthal symmetry is[3]

$$V(\zeta,\eta) = \sum_i\left\{AP_i(\zeta) + BQ_i(\zeta)\right\}\left\{A'P_i(\eta) + B'Q_i(\eta)\right\} \quad (12)$$

where Q_i is the ith Legendre polynomial of the second kind. We impose the boundary requirements:

put this as a maximum upper bound for the distortion due to a grounded object of elliptical cross section.

It is an oversimplification, however, to assume that the intruder remains at ground potential. For example, an initially grounded, conducting intruder has a charge distribution induced on his surface by the external field to enable him to remain at ground potential. Should the intruder break the connection to ground by lifting his feet, he reduces his capacity to ground which increases his potential. A similar if weaker effect occurs when the intruder picks each leg up, especially if his resistance to ground is not particularly high. Furthermore, scuffing shoes on the ground can lead to static charge being accumulated on the body, which must leak away in a finite time. The amount of charging is not inconsiderable. Over 20 years ago the Bureau of Mines[5] investigated the hazard of static electricity in operating theaters where there was danger of igniting explosive anesthetics. In a very comprehensive study it was shown that, depending upon the nature of the clothes, linens, furniture surfaces, shoes, and humidity in the room, potentials of 500-18000 volts could be generated on human beings. This charge leaked away through shoes with resistance of 10^5-10^9 ohms depending on the shoe material, which varies from partially conducting leather to highly insulating rubber. The time dependence of the potentials was also considered in that report. Thus, it becomes very necessary to obtain the field distortion due to a charged body. For this calculation we assume that the charged body is sitting on a thin insulating pad just above the ground.

Since the ground plane is at zero potential, one may resort to the theory of images to solve this problem. The application of this method to a charged conducting hemisphere on a ground plane leads to the well known exterior solution

$$V(r,\theta)=V_o\left[3/2\left(\frac{a}{r}\right)^3 P_1(\cos\theta)-7/8\left(\frac{a}{r}\right)^4 P_3(\cos\theta)+(11/16)\left(\frac{a}{r}\right)^6 P_5(\cos\theta)--\right] \quad (11)$$

where $P_i(\cos\theta)$ is the Legendre polynomial of the first kind. Again while the sphere is not a good approximation to the man, we can still use the same technique to solve the problem of the charged conducting prolate ellipsoid.

The general solution of the Laplacian in prolate spheroidal coordinates with azimuthal symmetry is[3]

$$V(\zeta,\eta) = \sum_i \left\{A P_i(\zeta) + B Q_i(\zeta)\right\}\left\{A' P_i(\eta) + B' Q_i(\eta)\right\} \quad (12)$$

where Q_i is the ith Legendre polynomial of the second kind. We impose the boundary requirements:

$$V(\zeta,\eta\to\infty) = 0; \quad V(\zeta,\eta_o) = \begin{cases} V_o, & 0 \le \zeta \le 1 \\ -V_o, & 0 \le \zeta \le -1 \end{cases}$$

Outside the spheroid only $P_i(\zeta)Q_i(\eta)$ is finite as $\eta\to\infty$, so Eqn. 12 reduces to

$$V(\zeta,\eta) = \sum_i A_i \, P_i(\zeta) \, Q_i(\eta) \tag{13}$$

where the Fourier coefficients are determined by

$$A_i = (2i+1) \, V_o[Q_i(\eta_o)]^{-1} \int_o^1 P_i(\zeta) d\zeta \tag{14}$$

Thus,

$$V(\zeta,\eta) = V_o\left\{3/2P_1(\zeta)\frac{Q_1(\eta)}{Q_1(\eta_o)} - 7/8P_3(\zeta)\frac{Q_3(\eta)}{Q_3(\eta_o)} + 11/16P_5(\zeta)\frac{Q_5(\eta)}{Q_5(\eta_o)} - \cdots\right\} \tag{15}$$

If the charged body is in a uniform externally applied field we simply superimpose the solutions of Eqn. 4 and Eqn. 15. We have numerically evaluated the potential distribution for several values of V_o both in and out of the earth's field. The vertical distortions are shown in Fig. 8. It may be seen that if the charge on the body is appreciable, then the distortion due to the earth's field is rather negligible compared to the distortion due to the charged body itself.

Time dependence may be included in the calculation in a straightforward way by considering the two effects described above. First, as the intruder approaches the sensor, the field distortion at the sensor will increase due to his increasing proximity. Second, as the intruder lifts his foot to walk, his potential will rise causing a change in field distortion at the sensor. The combination of these two effects produces a fluctuating field distortion at the sensor, which is considered to be the sensor input signal.

A model for the potential profile of the intruder was obtained in the following manner. Several people, each in turn holding a wire connected to an electrometer, walked slowly across the laboratory. Each person's potential profile was recorded. One of these profiles, shown in Fig. 9, was selected as the basis for the walking model. Note that the subject carries a negative potential due to his retention of electrons as he lifts his feet. Also, the large potential rise is due to the capacitance change as the subject lifts his foot. Smaller changes are attributed to the heel and toe motion as the subject shifts his weight.

For ease in calculation we simplified the profile of Fig. 9 by taking the profile to be periodic once walking commenced, and that local maxima and minima could be connected by straight lines. Vertical field distortion curves were plotted for the six intruder potentials corresponding to the local extrema. Using a measured velocity of .83

meter/sec, a period of 1.6 seconds, and an initial displacement of ten meters from the sensor, the person's displacement from the sensor at each potential maximum or minimum was calculated and marked on the appropriate distortion curve. Connecting these points with straight lines yielded the idealized triangular wave taken as the walking intruder sensor input model (Fig. 10).

The coupling of the field distortions through the atmosphere to the sensor is a complex process. An isolated electrically neutral wire placed in a potential gradient will distort the field such that it averages the field along its length. If the wire be connected to an electrometer, however, the small input capacitance to ground, leads to additional charge redistribution. Furthermore, the electrometer input resistance is not infinite so some leakage to ground will occur. The result of these phenomena is that the potential on the wire is lowered, or the effective height of the antenna is reduced.

In addition, there is a general atmospheric relaxation time for electrical phenomena due to the low but non-vanishing atmospheric conductivity. In a discussion given by Chalmers[6], it is shown that if a conductor of area A carries a charge Q and is exposed to the atmosphere, it leaks charge as given by Ohm's law $i = \lambda EA$. Close to the surface $E = Q/A\epsilon_o$; thus, $Q = \lambda Q/\epsilon_o$ and $Q = Q_o e^{-t/\tau}$ where $\tau = \epsilon_o/\lambda$ is the atmospheric relaxation time and λ is the atmospheric conductivity.

This relaxation time suggests as a model for the atmospheric coupling a parallel resistance capacitance combination which is connected to the electrometer. Thus, a reasonable candidate for an equivalent circuit is given in Fig. 11. For the output of the circuit to reflect the input with little lag, the time constant of the probe resistance and electrometer capacitance, rC, should be reasonably small. In addition, to reduce the voltage drop across the probe resistance, it should be small with respect to the detector resistance, R. Since R is specified to be 10^{14} ohms for state-of-the-art solid state (MOS/FET) electrometers, these conditions can be met by use of a radioactive probe which will reduce the probe resistance to 10^{10}-10^{12} ohm.

To obtain a value for the resistance of an ionization enhanced probe, an experimental sensor consisting of a state-of-the-art lab type electrometer with an enhanced wire probe was placed in a Faraday cage, and its response to a unit step change in electric field strength was recorded. The resulting curve was similar to that associated with the voltage rise across a capacitor placed in a series with a resistor and the input voltage. The electrometer is specified to have a capacitance of under five picofarads shunted by a very high

but finite (10^{14} ohm) resistance. Using these values and the experimentally measured response time, the probe resistance was calculated to be about 10^{11} ohms. The same experiment was simulated on the computer using the above values of the model parameters in the limit of the probe capacitance approaching zero. The results were quite comparable.

Sensor response to the input signal shown in Fig. 10 has been calculated for various values of the three sensor parameters. The output for two combinations of these is shown in Fig. 12. The smoothing effect of the larger electrometer input capacitance is evident. It is possible that under favorable ionization conditions, the probe resistance would fall to 2×10^{10} ohms. A model calculation using this value was made. The results, plotted in Fig. 13, clearly show the enhancement of structure in the sensor output signal.

EXPERIMENTAL STUDIES

To evaluate the feasibility of employing electrostatic means as an intrusion detection method, various state-of-the-art electrometers were considered with respect to their input resistance, capacitance and input offset current. When run open circuit, offset current will charge the probe and quickly saturate the electrometer. Due to its high input impedance and its particularly low offset current (less than 3×10^{-15} amp), the Princeton Applied Research Corp. PAR-135 electrometer was selected for further experimental work.

Two probe types were tested. One was simply a straight length of stainless steel tubing, 0.037 inch in diameter, projecting 10 cm from the input jack of the PAR-135. The other type was made from the same material projected 5 cm from the PAR-135, and had a small amount of Polonium fastened to the end.

Polonium ionizes the air in its immediate vicinity. The ionization provides a relatively rapid means for the probe to come to the same potential as the air around it, effectively decreasing the probe resistance. Decreased response time and increased sensitivity are the principal benefits obtained by its use. The enhancement produced by the Polonium is evident in the field test results discussed below.

Several field tests were made to determine the best sensor configuration to utilize in recording the response of these sensors to the intrusion of a person. To minimize possible electrostatic interference, these tests were conducted in open country fields.

To obtain an estimate of local field variations, two sensors

were placed on the ground. Sensor A was equipped with the 5 cm Polonium enhanced probe; Sensor B, 18 m away, with the 10 cm wire probe. Variations in the earth's electric field were monitored for twenty minutes by both sensors. Such disturbances as did occur appeared on both outputs, but more strongly on the output of the sensor with the Polonium probe, and were probably due to small clouds of ionized gas drifting over the field.

Sensor response to an intruder walking slowly toward it is shown in Fig. 14 for the enhanced probe and in Fig. 15 for the plain probe. The intruder's steps can be detected at about 8 meters with the enhanced probe, and at about 6½ meters with the plain probe. The output signal is stronger also for the enhanced probe, having changed by 170 mv at 3 m. while only by 100 mv at 3 m. for the plain probe.

In these measurements a bias was placed on the recorder in order to suppress the constant earth's field. Therefore, the zero volt reference line is not identified on these recordings, but it may be taken to be the line generated before the intruder nears the sensor, since only intruder induced distortions are of interest for comparison with the model calculation.

Plotting the computed sensor outputs on a linear scale, we find good agreement with the measured response. One of these linear plots, corresponding to an electrometer input capacitance of 1 pf is shown in Fig. 16. Although there is a scale factor of two between the voltage scales of Figs. 16 and 14, there is good correlation in the signature and rate of signal increase as the intruder approaches the sensor. There are several reasons for the presence of the scale factor, the most important of which is the fact that the potential profiles generated in the laboratory did not match the one used in the field.

Sensor response to the static presence of an intruder was approximated by instructing the intruder to pause five seconds between each step taken toward the sensor (See Fig. 17). Each step consists of a small signal as the intruder flexes his legs in preparation for the step, a large spike as he takes the step, and a second small signal as he relaxes. The signal is then fairly constant until the next step, but offset from its previous value. The offset is due only to the proximity of the intruder to the detector.

The last figure, Fig. 18, shows sensor response when the intruder was running in place at various distances from the sensor. It was determined the person used as the intruder in these experiments had very low resistance to ground. Any static charge built up by

walking would quickly leak off, leaving his body potential close to zero. By running in place, he could increase his resistance to ground and build up his potential, which would increase the effect on the sensor. Detection is easier to recognize in this case also because of the periodicity of the signal. As shown in the figure, he was detected by this sensor at 16 meters.

CONCLUSIONS

The results of preliminary experimental tests appear to verify analytical studies indicating that the characteristic signature of walking persons can be detected by sensors utilizing standard portable solid state electrometers equipped with simple 5 to 10 cm wire antennas. Field test data show detectability to ranges of 8 meters and more.

Future work will be directed toward further studies to establish the characteristics of background noise, optimum antenna configurations, and weather degradation. In addition, signal processing techniques will be studied to optimize sensor performance.

REFERENCES

1. W.R. Smythe, "Static and Dynamic Electricity", 2nd Edition, (McGraw-Hill, 1950).

2. P.M. Morse and H. Feshbach, "Methods of Theoretical Physics", (McGraw-Hill, 1953).

3. James Jeans, "Electricity and Magnetism", Fifth Edition, (Cambridge Press University Press, 1951).

4. I.S. Gradshteyn and I.W. Ryzhik, "Table of Integrals, Series and Products", (Academic Press, 1965).

5. P.G. Guest, V.W. Sikora, and B. Lewis, "Static Electricity in Hospital Operating Suites", Bureau of Mines Report of Investigations #4833, January 1952.

6. J.A. Chalmers, "Atmospheric Electricity", (Pergamon Press, 1957).

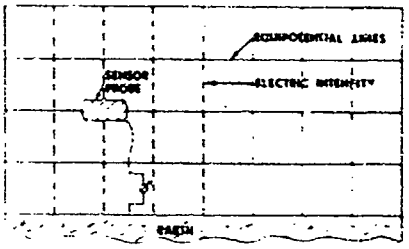

Fig. 1a. Undisturbed Earth's Electric Field

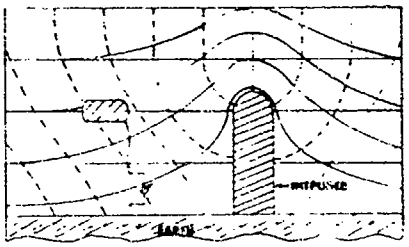

Fig. 1b. Disturbance of Earth's Field Due to Grounded Intruder

Fig. 2. Block Diagram of Intrusion Detection System

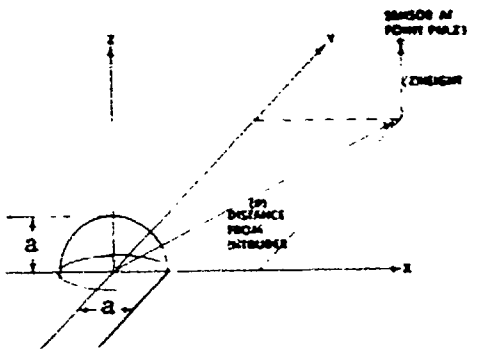

Fig. 3. Hemispherical Intruder Model

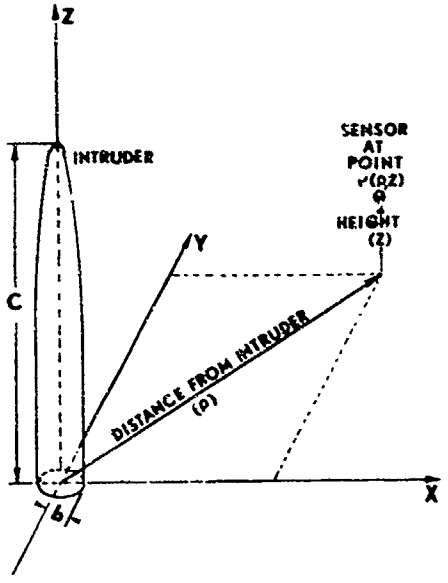

Fig. 4. Hemi-prolate Spheroid Intruder Model which is Closer to the True Proportions of a Person

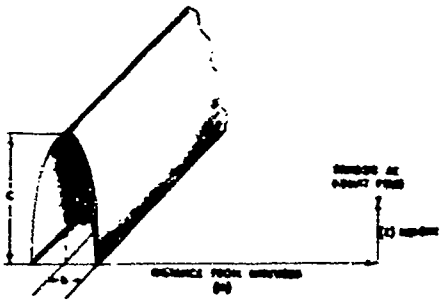

Fig. 5. Hemi-Elliptic Cylinder Representing an Upper Limit to Intruder Size

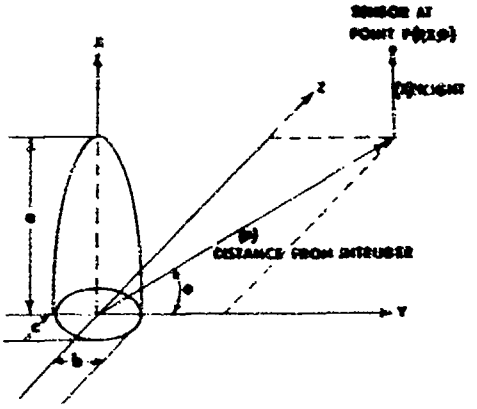

Fig. 6. Hemi-Ellipsoid which allows for the Intruder's Lack of Rotational Symmetry

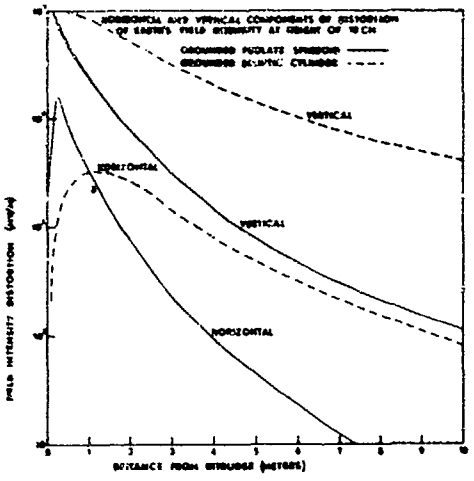

Fig. 7. Comparison of Field Distortions Due to Crounded Prolate Spheroid and Elliptic Cylinder

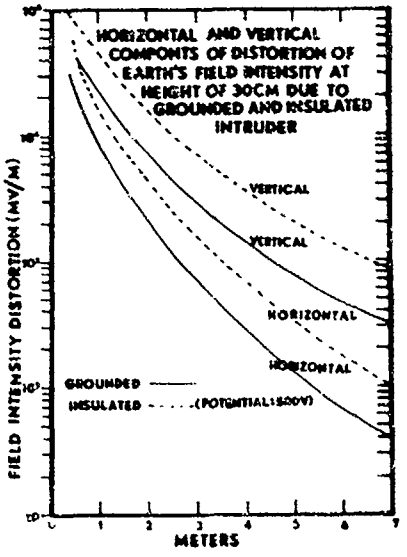

Fig. 8. Comparison of Field Distortions Due to Grounded and Insulated Intruder Using the Prolate Spheroid Model

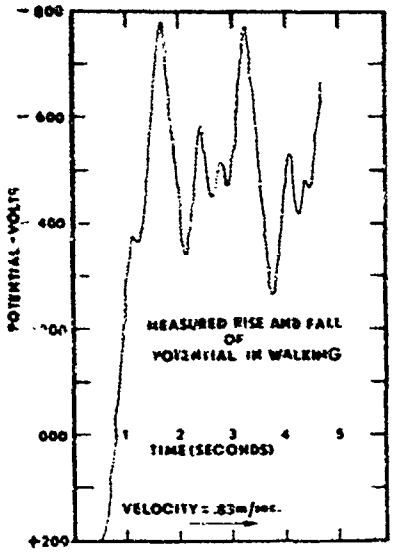

Fig. 9. Laboratory Measurement of the Potential Profile Due to the Rise and Fall of the Feet While Walking

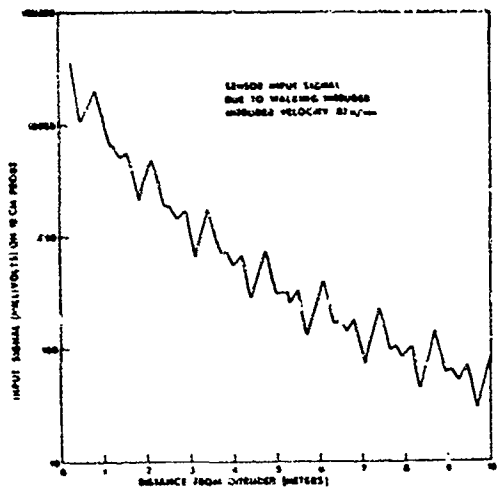

Fig. 10. Input Signal Due to Walking Intruder

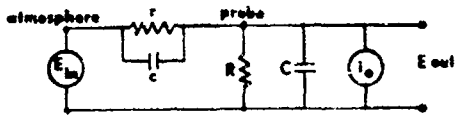

E_{in}: sensor input signal
r : probe resistance
R : electrometer resistance
C : electrometer capacitance
c : probe capacitance
E_{out}: electrometer output signal
i_o : input offset current

Fig. 11. Equivalent Circuit for Sensor Input Signal, Atmospheric Coupling, and Detector Input Impedance

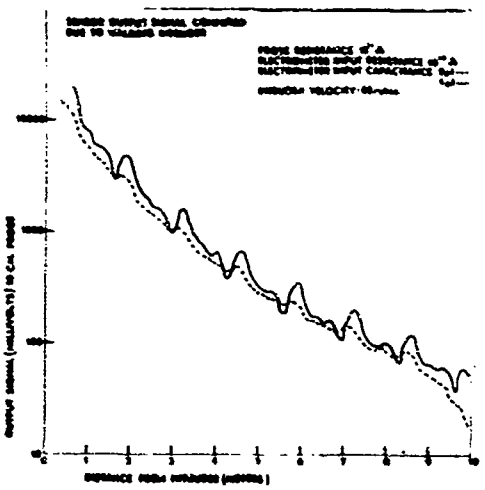

Fig. 12. Computed Sensor Output for Two Values of Electrometer Capacitance Using an Enhanced Zero Capacitance Probe

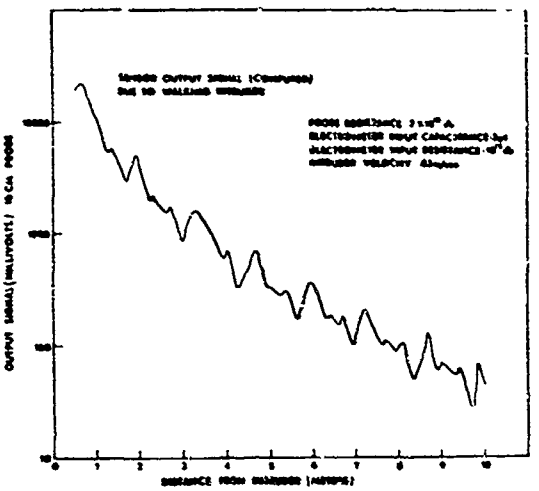

Fig. 13. Computed Sensor Output Signal for a Highly Enhanced Probe

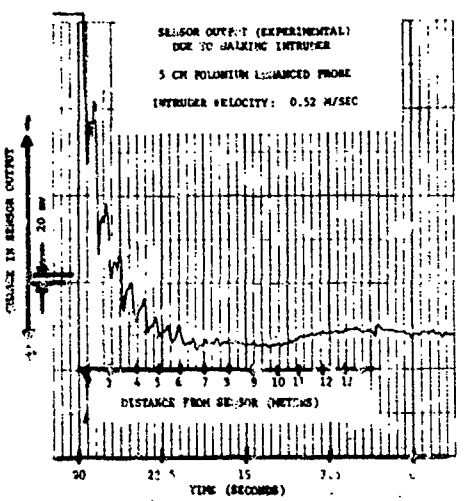

Fig. 14

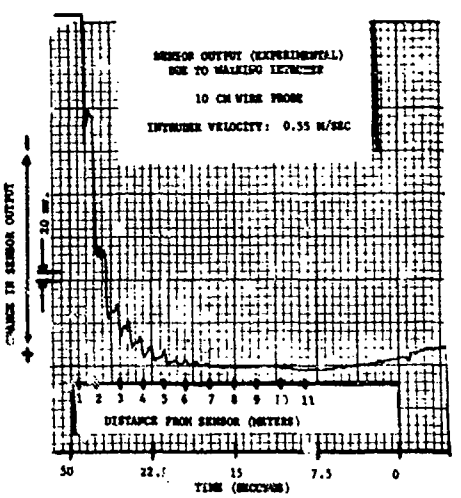

Fig. 15

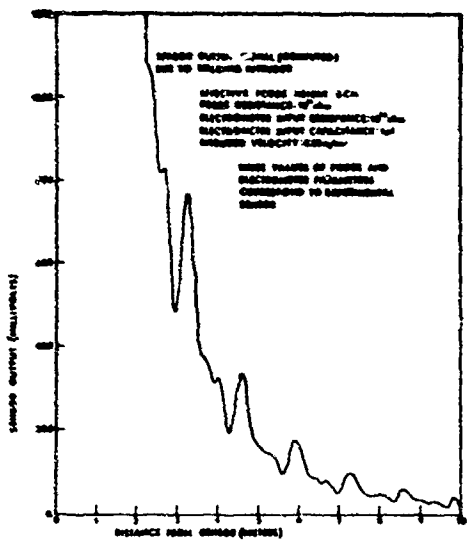

Fig. 16. Computed Sensor Output Plotted on a Linear Scale for Ease in Comparison with Experimental Data in Fig. 14

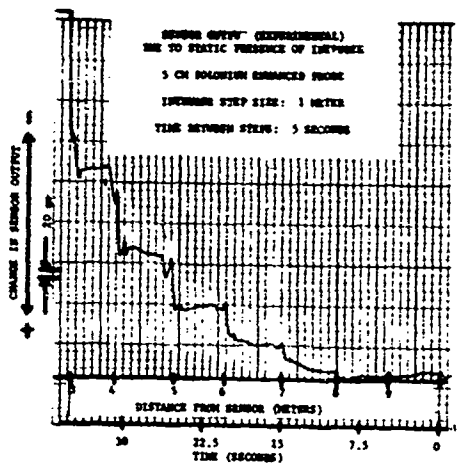

Fig. 17

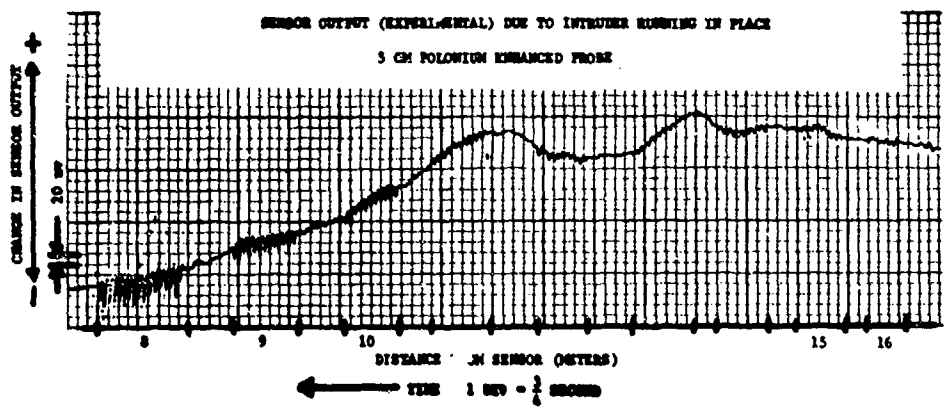

Fig. 18